JASMAC
Conference of the Japan Society of Microgravity Application

OS4-6

静電浮遊炉を用いた模擬スペースデブリに発生するレーザーアブレーション推力の測定

Measurement of laser ablation thrust generated in simulated space debris using an electrostatic levitation reactor

皆川尚樹 [1], 森浩一 [1], 石川毅彦 [2], 小山千尋 [2]
Naoki MINAGAWA[1], Koichi MORI[1], Takehiko ISHIKAWA[2], and Chihiro KOYAMA[2]
[1] 大阪公立大学 , Affiliation of author group#1,
[2] 宇宙航空研究開発機構, Affiliation of author group#2,

1. Introduction

In recent years, the increase in space debris has become a major problem in space development. Space debris orbiting the earth comes in all sizes. In this study, we consider the removal of debris smaller than 10 cm[1)], which is difficult to observe and impossible to avoid debris collisions through orbit control. Orbital transformation by laser ablation thrust is promising for such debris removal below 10 cm.[2)] In the case study by Ebisuzaki [3)] , debris is detected and its motion state is acquired using an ultra-wide angle telescope and a search laser beam, and based on this information, nanosecond Based on this information, a scenario to deactivate debris of about 1-10 cm in size by repeated irradiation of pulsed lasers with a time-averaged power of 500 kW is proposed. When such high-power lasers are irradiated to such small space debris as described above, most of the debris melts and turns into droplets. Based on the results of recent studies, it is feared that irradiating the droplets with a laser beam will cause them to break up, resulting in further debris growth. Therefore, our laboratory is considering a method to avoid debris breakup by using a low-power-density laser to thrust. However, for practical use, the laser ablation thrust acting on actual debris must be estimated. Previous experiments have used target materials that are sufficiently large for the thermal input and do not simulate thermo-mechanical isolation.[2)] Under these conditions, the thruston space debris in space cannot be accurately measured. In this study, we used an electrostatic levitation furnace, which can create a thermomechanical isolated, and vacuum environment by levitating a sample using electrostatic force, to measure the thrust generated by irradiating a Zr, Ti, and SUS metal sphere with a diameter of approximately 2 mm, which simulates space debris, with a laser. In this experiment, a CW laser beam was irradiated because it is considered difficult to bring a large-power laser such as a pulsed laser into space.

2. Experimental Methods

2.1. experimental equipment

In this study, experiments were conducted using a high-vacuum electrostatic levitation furnace[4-7] owned by the Ishikawa Laboratory, Department of Interdisciplinary Chemistry, Institute of Space and Astronautical Science, JAXA. Figure 1 shows a schematic diagram of the electrostatic levitation furnace. The electrostatic levitation furnace uses the electrostatic levitation method, in which levitation is achieved by the Coulomb force between the charged sample and the upper and lower electrodes and is capable of holding the sample without a container and melting it without contact.

The sample must be charged when levitating, since electrostatic force is used to levitate the sample. In the initial levitation process, the specimen is positively charged by bringing it into contact with the bottom electrode, and to maintain the specimen's charge after levitation, the specimen is irradiated with ultraviolet light during heating to increase its positive charge by utilizing the photoelectric effect. Furthermore, during laser irradiation, the positive charge is increased due to the emission of thermionic electrons when the sample becomes hot. By maintaining the amount of charge on the sample in this manner, sustained levitation is possible.

In order to maintain stable levitation in the electrostatic levitation method, the voltage between the upper and lower electrodes is adjusted by PID control based on the sample position information detected by the PSD (Position Sensitive Detector) and IVS (Intelligent Vision Sensor), which are position detectors. The PID control is a high-speed feedback control that adjusts the voltage between the upper and lower electrodes.

As shown in Figure 1, the bottom electrode plate has a diameter of 25 mm and the top electrode plate has a diameter of 10 mm, which allows stable levitation in the horizontal direction due to the Coulomb force acting between the top and bottom electrodes. The electrodes in the horizontal direction are also orthogonal to each other, and the Coulomb force applied in the horizontal direction is controlled by high-speed feedback through PD control, enabling stable levitation in the horizontal direction. The stable levitation is shown in Figure 2.

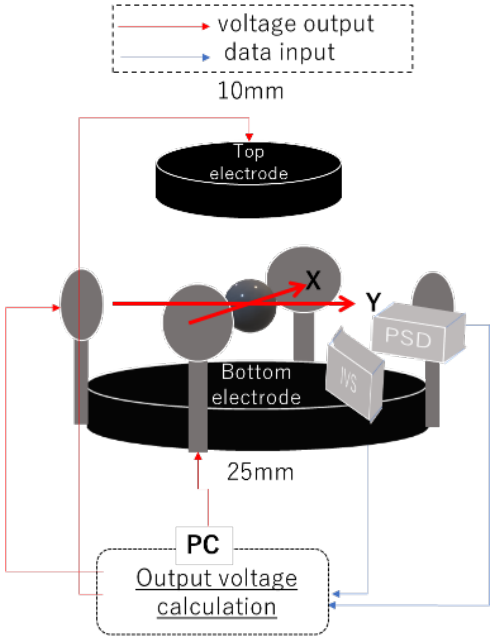

Figure 1. Schematic diagram of electrostatic levitation

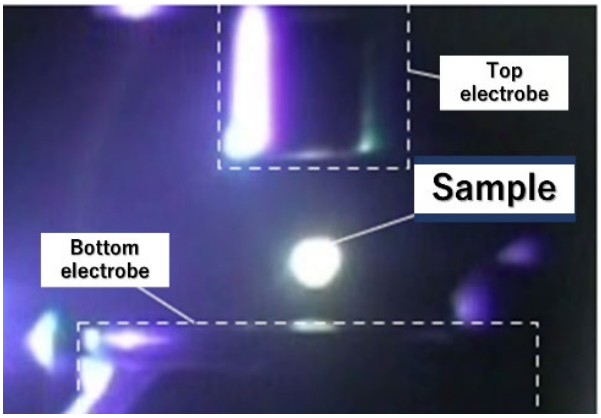

Figure 2. Floating Sample in the ELF

2.2 Experimental Procedure

First, the sample was heated and melted by irradiating it uniformly from three directions with a carbon dioxide laser beam (wavelength 10.6 μm, maximum power 100 W, SYNRAD Firestar series V40). Next, of the three laser beams, only one laser beam is left and the other two are cut off. After this, the laser power was increased and then decreased after a certain period of time, repeatedly irradiating the sample in pulses, and the behavior of the sample was observed with a camera. Aluminum should be used to simulate space debris, but aluminum is difficult to melt and levitate in an electrostatic levitation furnace on the ground, so Zr, Ti, and SUS were used for stable levitation. Experiments on aluminum are planned to be conducted on the International Space Station. The pressure in the chamber was reduced to about $10^{-4}[Pa]$ by a vacuum pump. The temperature of the samples was measured with a radiation thermometer (IR-CA-Q8C5 monochromator (measurement range: 500-3500°C) manufactured by Chino Corporation).

2.3. Motion model of the sample

Take the x-axis and y-axis as shown in Fig. 1. Let k be the effective spring constant of the restoring force, k_P be the proportional gain by PD control, k_D be the differential gain by PD control, x_0 and y_0 be the target values of control, and F_x and F_y be the thrust by laser ablation in x and y directions, respectively, the equations of motion in x and y directions are

$$\begin{cases} m\ddot{x} + k_{Dx}\dot{x} + (k + k_{Px})(x - x_0) = F_x \\ m\ddot{y} + k_{Dy}\dot{y} + (k + k_{Py})(y - y_0) = F_y \end{cases} \quad (1)$$

Consider the x-axis. Solving Eq. (1) , turn out as follows

$$x = Xe^{-\frac{k_{Dx}}{2m}t}\cos\left(\sqrt{\frac{k + k_{Px}}{m} - \frac{{k_{Dx}}^2}{4m^2}}t + \alpha\right) + \Delta x \quad (2)$$

where Δx is the change from the neutral position. Then, the thrust F_x is derived as follows

$$F_x = (k + k_{Px})\Delta x \quad (3)$$

From the Eq. (3), the running spring constant $(k + k_{Px})$ and the neutral position change Δx is necessary to measure the spring constant.

2.4. Estimation method for thrust and momentum coupling coefficients

First, let us discuss how to obtain the running spring constant $(k + k_{Px})$. Since it is calculated in the same way in the x- and y-directions, we will discuss the x-direction here as well. Figure 3 shows the position change data measured by PSD and IVS after laser irradiation. Figure 4 shows that damped oscillations are observed after laser irradiation. The natural frequency f_x and the damping coefficient k_{Dx} were obtained by fitting the damped vibration. The fitting results are shown in Figure 4. From these values

$$2\pi f_x = \sqrt{\frac{k + k_{Px}}{m} - \frac{{k_{Dx}}^2}{4m^2}} \qquad (4)$$

The effective spring constant was derived using the equation

Next, the method for obtaining the change in neutral position Δx is described. It is known that the PSD and IVS data contain low-frequency noise and that the neutral position has drifted. Therefore, displacement data were obtained by analyzing video images of a camera observing the sample from the positive direction of the z-axis. In the image analysis, a circle was detected using the Hough circle detection method, the coordinates of the center were extracted, and the displacement was measured.

Next, we describe the method used to measure the thrust at each time point.

The momentum coupling coefficient C_m [N/GW] was obtained by integrating the thrust obtained as described above, obtaining the force product, and then dividing by the energy given to the sample by the laser, using the following formula. The thrust was $F(t)$ [N], and the laser was irradiated at a power of P_l[GW] from time 0[s] to t_i [s].

$$C_m = \frac{\int_0^{t_i} F(t)dt}{P_l t_i}\left[\frac{N}{GW}\right] \qquad (5)$$

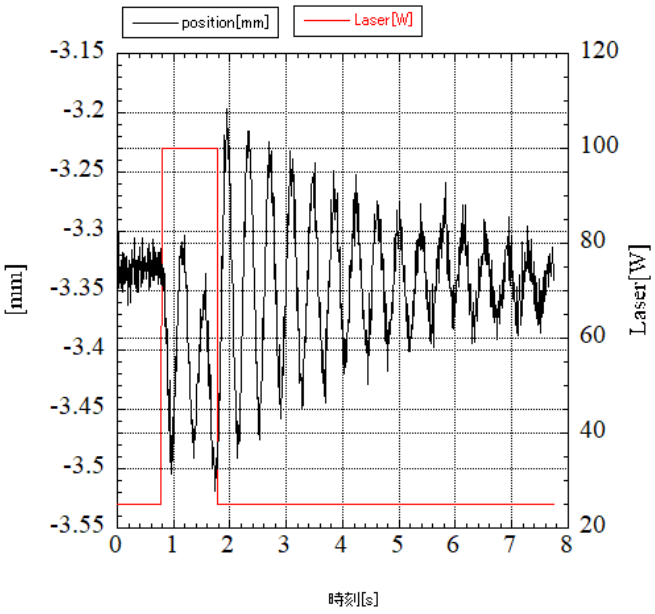

Figure 3. Schematic diagram of electrostatic levitation

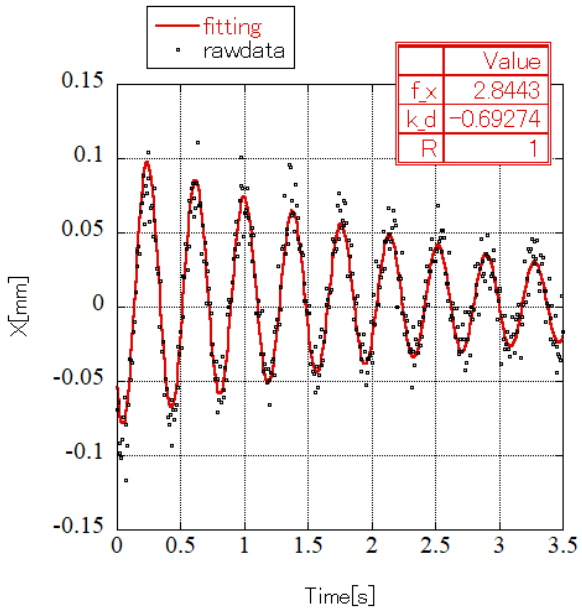

Figure 4. Damping vibration fitting results

3. Experimental Results and Discussion

3-1. Experimental Case

I show the experiments conducted in Table 1.

3-2. Variation of thrust with time

Figure 5-7. shows the time variation of the thrust for #1, #3, and #4 of Table1 as the laser output is varied. The dotted lines are the results obtained from Equation (3) based on the data obtained by image processing and the running spring constant of $6.41 \times 10^{-3}[N/m]$ [N/m] obtained from Figure 4. The solid line in the figure is the result obtained from the result in Figure 4 by considering the natural frequency and performing a moving average over the period. The red line indicates the laser output.

Figure 5 shows that in the case of Zr, the thrust reaches a constant value about 0.7[s] after the laser power increases. Similarly, Figure 6 shows that in the case of Ti, the thrust reaches a constant value about 0.6[s] after the laser power increases. On the other hand, Figure 7 shows that the thrust is not constant for SUS. We will discuss the cause of this. The thermal conductivities of the three materials are 94.61[W/(m・K)] [8], 27.2[W/(m・K)] [9], and 17.81[W/(m・K)] [10] for Zr, Ti, and SUS, respectively, near the melting point of the sample. This is indicating that only SUS is smaller than the other two materials. This indicates that the larger the thermal conductivity, the earlier the steady state is reached and the earlier the thrust reaches the steady state. Therefore, it can be said that the way in which the thrust rises differs depending on the thermal conductivity of the material.

Table1. Experimental Case

Experiment Case	sample	Mass [mg]	Radius [mm]
#1	Zr	23.565	0.952
#2	Zr	24.576	0.965
#3	Ti	8.187	0.757
#4	SUS	32.664	0.994

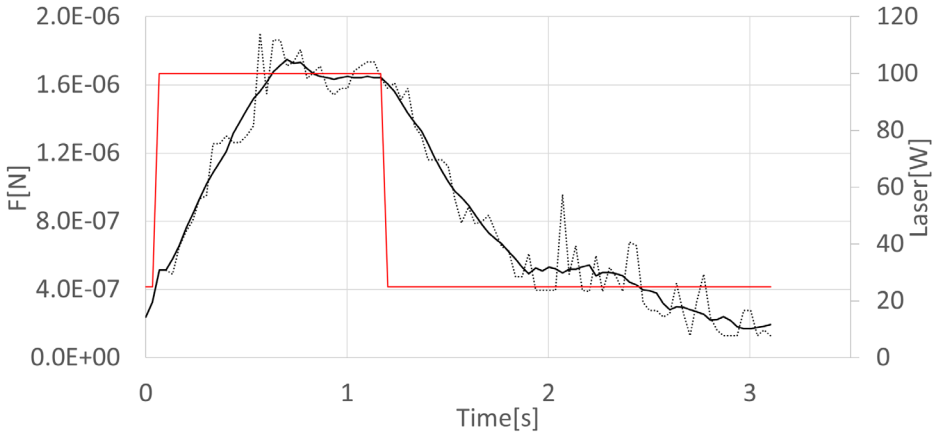

Figure 5. Variation of thrust with time of Zr

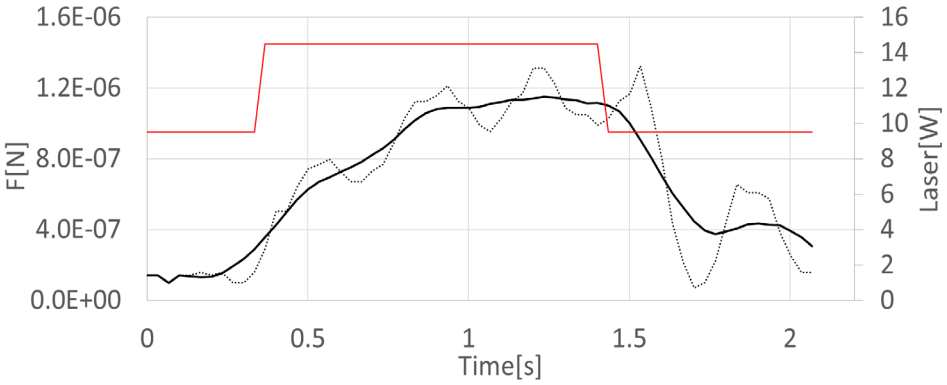

Figure 6. Variation of thrust with time of Ti

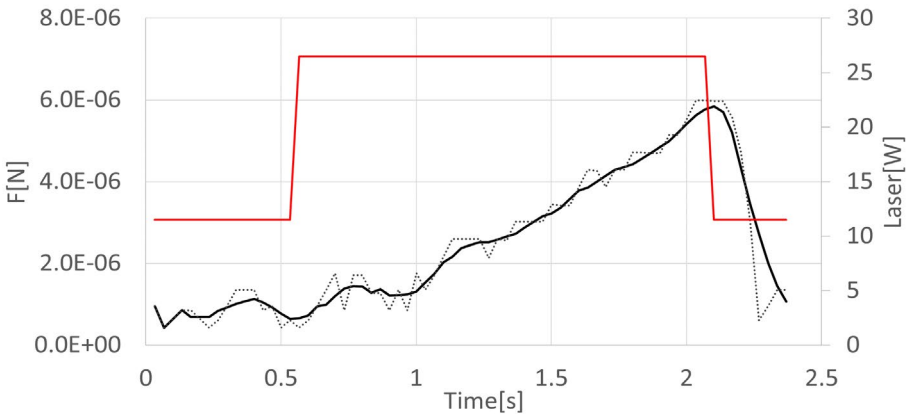

Figure 7. Variation of thrust with time of SUS

3-3. Material dependence of laser ablation thrust

The momentum coupling coefficients of these experiments in Table. 1 are summarized in Figure 8.

Figure. 6. shows that the momentum coupling coefficient increases in the order of Zr, Ti, and SUS. In the case of Zr, as mentioned above, there are differences in the magnitude of the momentum coupling coefficient depending on the sample used.

This may be because the thrust from laser ablation is thought to be generated by changes in vapor pressure. In fact, the temperatures of Zr, Ti, and SUS during laser irradiation were about 2200[K], 1950[K], and 1660[K], respectively, and their vapor pressures were 0.011[Pa], 0.50[Pa], and 0.60[Pa]. The order is consistent with the ascending order of the thrust obtained from the experimental results.[10,11] And the characteristics of vapor pressure in relation to temperature vary depending on the material, and that the local temperature varies depending on the sample and material because the laser absorption rate varies depending on the sample.

4.Conclusion

In this series of experiments, it became clear that the thrust by laser irradiation in space depends on the material.

Therefore, in future space experiments, it is necessary to analyze data using aluminum, which is the main component of space debris, to estimate the thrust acting on the debris.

In addition, there is a lot of variation in the data. Therefore, it is necessary to improve the reliability of the data by conducting more experiments in the future.

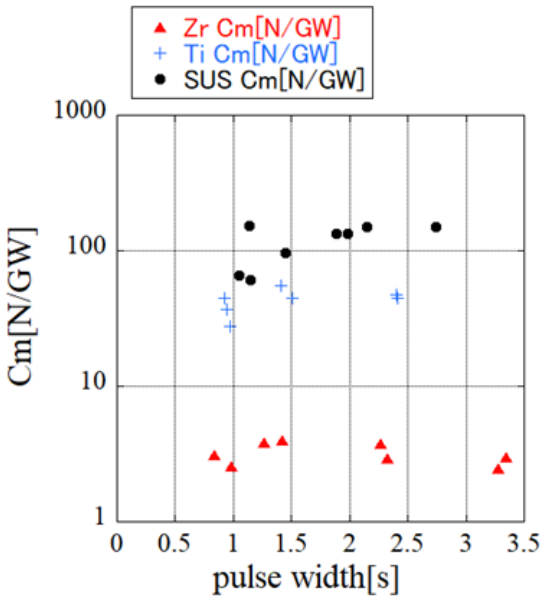

Figure 8. Summarize of Cm

Acknowledgments

I would like to thank the researchers at JAXA's Ishikawa Laboratory for allowing us to use their electrostatic levitation furnace as an experimental device, for their advice and cooperation on experimental methods, and for giving us the opportunity to conduct on-orbit experiments on the ISS. I would like to take this opportunity to express our deepest gratitude.

References

1) Kawamoto, Satomi et al. Overview of Space Debris Removal. Proceedings of the 56th Space Science and Technology Conference, 2012
2) The Institute of Electrical Engineers of Japan. Laser Ablation and its Applications. Corona, 1999.
3) Ebisuzaki, S., T. Wada, A. Sasou, et al. Space Debris Deorbit by Laser. JAXA Special Publication: 7th Space Debris Workshop Proceedings, 2017.
4) H. Tamaru, C. Koyama, H. Saruwatari, Y. Nakamura, T. Ishikawa and T. Takada: Status of the electrostatic levitation furnace (ELF) in the iss-kibo. Microgravity Sci. Technol., Vol. 30 (2018), No. 5, pp. 643-651.
5) T. Ishikawa, C. Koyama, H. Tamaru, H. Saruwatari, M. Ohshio and Y. Nakamura: Status of the Electrostatic Levitation Furnace in the ISS -Evaluation of Sample Posit0ion Control-. Int. J. Microgravity Sci. Appl., 35 (2018), No. 2, p. 350205
6) T. Ishikawa, P. -F. Paradis and T. Masaki: The electrostatic leviation method: accomplishments and challenges for the future, Space Utiliz. Res., 22, 2006.
7) ISHIKAWA, Takehiko. Measurement of Thermophysical Properties of High-Temperature Melts by Electrostatic Levitation Furnace. Materia, Vol. 45, No. 7, pp. 520-522, 2006.
8) Paul-Fran¸cois Paradis and Won-Kyu Rhim. Thermophysical properties of zirconium at high temperature. Journal of materials research, Vol. 14, No. 9, pp. 3713–3719, 1999.
9) K Zhou, HP Wang, J Chang, and B Wei. Experimental study of surface tension, specific heat and thermal diffusivity of liquid and solid titanium. Chemical Physics Letters, Vol. 639, pp. 105–108, 2015
10) C S Kim. Thermophysical properties of stainless steels.
11) CB Alcock, VP Itkin, and MK Horrigan. Vapor pressure equations for the metallic elements: 298–2500k. Canadian Metallurgical Quarterly, Vol. 23, No. 3